

Atomic Clock States of Thulium have Near-Zero Electric Quadrupole Moment

Timo Fleig*

*Laboratoire de Chimie et Physique Quantiques,
FeRMI, Université Paul Sabatier Toulouse III,
118 Route de Narbonne, F-31062 Toulouse, France*

(Dated: February 6, 2023)

Abstract

A method for highly accurate calculations of atomic electric quadrupole moments (EQM) is presented, using relativistic general-excitation-rank configuration interaction wavefunctions based on Dirac spinors. Application to the clock transition states of the thulium atom employing up to full Quadruple excitations for the atomic wavefunction yields a final value of $Q_{zz}(^2F_{7/2}) = 0.07 \pm 0.07 \text{ a.u.}$, establishing that the thulium electronic ground state has an exceptionally small EQM. A detailed analysis of this result is presented which has implications for EQMs of other atoms with unpaired f electrons.

* timo.fleig@irsamc.ups-tlse.fr

I. INTRODUCTION

In atomic systems electric quadrupole moments of the electron shells are of importance in the quest for setting new standards of time measurement. In fact, they are often one of the limiting quantities in optical atomic clock's fractional frequency uncertainty [1]. The reason for this type of uncertainty is that in many implementations of atomic clocks an environmental perturbation, a residual external electric-field gradient, interacts with the EQM of the (atomic) charge distribution in the relevant clock-transition states, giving rise to the so-called “quadrupole shifts” [2] of atomic energy levels.

Lanthanide atoms have electronic valence shells $4f^k$ where the k f electrons are partially shielded from external electric fields by the electrons occupying the $6s$ shell. This makes $f - f$ transitions in lanthanides less susceptible to EQM interactions with the gradients of an external electric field [3]. Indeed, great progress has very recently been made in devising a transportable optical clock using the hyperfine levels of the ground-state $f - f$ transition in thulium atoms [4–7]. The EQM interaction is nevertheless one of the sources of uncertainty in this type of atomic clock. However, electronic properties of lanthanide atoms are notoriously difficult to calculate accurately.

The method of calculating EQMs presented in this paper is based on relativistic configuration interaction (CI) wavefunctions of general excitation rank, up to the level of Full CI [8]. The implementation is highly efficient, allowing for CI expansions with up to 10^{10} (10 billion) linear expansion terms and thus for very accurate calculation of electron correlation effects. This will be demonstrated in the present paper. Moreover, the present approach is particularly advantageous when atomic states with complicated shell structure – such as with several unpaired d and/or f electrons – have to be addressed [9]. The present approach is also directly applicable to molecules.

The article is structured as follows: In section II the theory of the atomic electric quadrupole moment is briefly reviewed and the present implementation using relativistic configuration interaction (CI) wavefunctions for electronic ground and excited states is described. The same method is in the present also applied in the calculation of the magnetic hyperfine interaction constant. Section III contains the applications, first to the beryllium (Be) atom as a test system for verification of the present implementation, then to the radium mono-cation (Ra^+) as a more complex system where relativistic effects are strong. Finally, predictions are made for EQMs of ground and excited states of the thulium (Tm) atom, in the case of excited states of Tm for the first time. In the final section IV conclusions from the present findings are drawn.

II. THEORY

A. Interaction energy

An arbitrary charge distribution immersed in an external electric field \mathbf{E} gives rise to an electrostatic interaction energy [10], the second-order term of which is written out as

$$W_2 = -\frac{1}{6} \sum_{i,j} Q_{ij} \left. \frac{\partial E_j(\mathbf{x})}{\partial x_i} \right|_{\mathbf{x}=\mathbf{x}_0} \quad (1)$$

where \mathbf{x}_0 is some conveniently chosen expansion point, \mathbf{Q} is the rank-2 electric quadrupole moment tensor of the charge distribution and $\frac{\partial E_j(\mathbf{x})}{\partial x_i}$ is a component of the electric-field gradient. In the present case the charge distribution is represented by the electron shells of the atomic systems under consideration. The atomic nucleus is described by a spherical Gaussian charge distribution and thus does not contribute to the EQM of the atom.

B. Atomic electric quadrupole moment

The relevant element of the rank-2 tensor Q of the atomic electric quadrupole moment has been defined as [2, 11, 12], in *a.u.* ,

$$Q_{zz} := \left\langle \Psi \left| -\sum_{i=1}^n \sqrt{\frac{4\pi}{5}} r^2(i) Y_{2,0}(\vartheta, \varphi) \right| \Psi \right\rangle \quad (2)$$

with Ψ the atomic wavefunction, n the number of electrons, r the radial electron coordinate and Y_{ℓ, m_ℓ} a spherical harmonic. In Condon-Shortley convention we have

$$Y_{2,0}(\vartheta, \varphi) = \frac{1}{4} \sqrt{\frac{5}{\pi}} (3 \cos^2(\vartheta) - 1) \quad (3)$$

Therefore,

$$Q_{zz} = -\frac{1}{2} \left\langle \Psi \left| \sum_{i=1}^n r^2(i) (3 \cos^2(\vartheta) - 1) \right| \Psi \right\rangle \quad (4)$$

An elementary coordinate transformation yields

$$r^2 (3 \cos^2(\vartheta) - 1) = 2z^2 - x^2 - y^2 \quad (5)$$

in terms of cartesian coordinates, and so

$$\begin{aligned} Q_{zz} &= -\frac{1}{2} \left\langle \Psi \left| \sum_{i=1}^n (2z^2(i) - x^2(i) - y^2(i)) \right| \Psi \right\rangle \\ &= -\frac{1}{2} \left\{ \left\langle \Psi \left| \sum_{i=1}^n 2z^2(i) \right| \Psi \right\rangle - \left\langle \Psi \left| \sum_{i=1}^n x^2(i) \right| \Psi \right\rangle - \left\langle \Psi \left| \sum_{i=1}^n y^2(i) \right| \Psi \right\rangle \right\} \quad (6) \end{aligned}$$

The tensor element is evaluated by calculating the three resulting matrix elements over cartesian one-electron operators, the “second moments”. In the present case, however, $|\Psi\rangle \equiv |\alpha J M_J\rangle$ is a relativistic atomic Dirac wavefunction where α represents quantum numbers other than the total angular momentum J . Since a linear symmetry double group (in the present case D_{32h}^* which is an abelian subgroup of $D_{\infty h}^*$) is used instead of full rotational atomic symmetry the wavefunctions are obtained for individual M_J states. In practice, J for a given eigenvector is inferred by calculating a sufficient number of degenerate eigenvectors in the different relevant M_J subspaces. The individual states are represented by relativistic configuration interaction wavefunctions

$$|\alpha J M_J\rangle \equiv \sum_{I=1}^{\dim \mathcal{F}^t(M,n)} c_{(\alpha,J,M_J),I} (\mathcal{S}\overline{\mathcal{T}})_I | \rangle \quad (7)$$

where $\mathcal{F}^t(M,n)$ is the symmetry-restricted sector of Fock space with n electrons in M four-spinors, $\mathcal{S} = a_i^\dagger a_j^\dagger a_k^\dagger \dots$ is a string of spinor creation operators, $\overline{\mathcal{T}} = a_l^\dagger a_m^\dagger a_n^\dagger \dots$ is a string of creation operators of time-reversal transformed spinors. The determinant expansion coefficients $c_{(\alpha,J,M_J),I}$ are generally obtained as described in refs. [13, 14] by diagonalizing the Dirac-Coulomb Hamiltonian (in *a.u.*)

$$\hat{H}^{\text{Dirac-Coulomb}} = \sum_j^n \left[c \boldsymbol{\alpha}_j \cdot \mathbf{p}_j + \beta_j c^2 - \frac{Z}{r_j} \mathbb{1}_4 \right] + \sum_{j,k>j}^n \frac{1}{r_{jk}} \mathbb{1}_4 \quad (8)$$

in the basis of the states $(\mathcal{S}\overline{\mathcal{T}})_I | \rangle$, where the indices j, k run over electrons, Z is the proton number, and $\boldsymbol{\alpha}, \beta$ are standard Dirac matrices. The framework for the present implementation is the relativistic electronic-structure program package DIRAC [15] where a locally modified version of the code is used.

In the present paper the electric quadrupole tensor component is evaluated for the microstate with $M_J = J$, *i.e.*,

$$Q_{zz} = -\frac{1}{2} \left\langle \alpha J J \left| \sum_{i=1}^n (2z^2(i) - x^2(i) - y^2(i)) \right| \alpha J J \right\rangle. \quad (9)$$

based on the evaluation of properties using relativistic CI wavefunctions as described in Refs. [8, 16]. From the EQM expectation value for a given eigenvector with defined M_J the EQM for the other M_J -components of the associated state J can be calculated *via* the reduced matrix element (RME) evaluated through the adapted form of the Wigner-Eckhart theorem:

$$\text{RME} = \langle \alpha J || \hat{Q}_{zz} || \alpha J \rangle = \frac{\langle \alpha J M_J | \hat{Q}_{zz} | \alpha J M_J \rangle \sqrt{2J+1}}{\langle J 2 M_J 0 | J 2 J M_J \rangle} \quad (10)$$

where $\hat{Q}_{zz} = -\frac{1}{2} \sum_{i=1}^n [2z^2(i) - x^2(i) - y^2(i)]$ and α denotes quantum numbers other than those of total electronic angular momentum J . The Clebsch-Gordan coefficients

(CGC) in the denominator of Eq. (10) are calculated according to Wigner's (1959) general definition [17] as given in reference [18]:

$$\begin{aligned} \langle j_1 j_2 m_{j_1} m_{j_2} | j_1 j_2 j m_j \rangle &= \delta(m_j, m_{j_1} + m_{j_2}) \sqrt{\frac{(j_1 + j_2 - j)! (j + j_1 - j_2)! (j + j_2 - j_1)! (2j + 1)}{(j + j_1 + j_2 + 1)!}} \\ &\times \sum_k \frac{(-1)^k \sqrt{(j_1 + m_{j_1})! (j_1 - m_{j_1})! (j_2 + m_{j_2})! (j_2 - m_{j_2})! (j + m_j)! (j - m_j)!}}{k! (j_1 + j_2 - j - k)! (j_1 - m_{j_1} - k)! (j_2 + m_{j_2} - k)! (j - j_2 + m_{j_1} + k)! (j - j_1 - m_{j_2} + k)!} \end{aligned} \quad (11)$$

C. Magnetic Hyperfine Interaction

The magnetic hyperfine interaction constant has been implemented in the present electronic-structure methods as described in Refs. [19, 20]. For n electrons in the field of nucleus K it is defined in *a.u.* as

$$A(K) = -\frac{\mu_K [\mu_N]}{2cI m_p M_J} \langle J M_J | \sum_{i=1}^n \left(\frac{\boldsymbol{\alpha}_i \times \mathbf{r}_{iK}}{r_{iK}^3} \right)_z | J M_J \rangle \quad (12)$$

where μ_K is the nuclear magnetic moment, $\frac{1}{2cm_p}$ is the nuclear magneton in *a.u.*, m_p is the proton rest mass, I is the nuclear spin quantum number, and \mathbf{r} is the electron position operator.

III. APPLICATIONS AND RESULTS

A. Be

1. Technical details

The Gaussian basis set for Be is cc-pV6Z with added diffuse functions from the set aug-cc-pV5Z [21], amounting to $\{17s, 10p, 6d, 5f, 4g, 3h, 1i\}$ uncontracted functions. Spinors are optimized for the closed-shell ground state ($1s^2 2s^2$). A cutoff energy of 100 *a.u.* is used for the virtual spinor set. A Full CI expansion is used which includes the entire set of Triple and Quadruple excitations, amounting to ≈ 29 million Slater determinants.

2. Results and discussion

The above-defined model yields $Q_{zz}(2s^1 2p^1; {}^3P_2) = 2.2721$ *a.u.* for this Be excited state. For comparison, the four-electron limit result from Ref. [11] is $Q_{zz}(2s^1 2p^1; {}^3P_2) = 2.265$ *a.u.* This differs from the present result by only roughly 0.3% confirming the

reliability of the present implementation. The small difference is not explained by relativistic effects which had been found to be smaller than 0.01% but rather by the fact that in Ref. [11] a finite-element method is used whereas in the present case a finite Gaussian basis set is employed.

As a further consistency test $Q_{zz}(2s^1 2p^1; ^3P_2, M_J = 1) = -1.136 \text{ a.u.}$ is calculated explicitly from the relevant M_J eigenvector. The value for $Q_{zz}(2s^1 2p^1; ^3P_2, M_J = 1)$ but calculated from $Q_{zz}(2s^1 2p^1; ^3P_2, M_J = 2)$ and $\text{RME}(2s^1 2p^1; ^3P_2)$ obtained from Eq. (10) is indeed identical.

B. Ra^+

1. Technical details

For Ra^+ a Gaussian basis set of quadruple-zeta quality is used where all $\{6s, 6p, 7s, 7p\}$ -correlating and all dipole-polarizing primitive functions have been included [22]. The Dirac spinors are optimized by diagonalizing a Fock operator where a fractional occupation of $f = \frac{1}{12}$ per $7s$ and $6d$ spinor is used. Effectively, this yields a Dirac-Hartree-Fock state that is averaged over the $^2S_{1/2}$ ground term and the $^2D_{3/2,5/2}$ excited terms with spinors that are not biased towards any of the corresponding states. In correlated models the nine outermost electrons from shells $6s, 6p, 7s$ are considered.

2. Results and discussion

EQMs and level energies for Ra^+ are compiled in Table I. The DCHF results using spinors specific to the electronic ground state of Ra^+ ($7s^1$ configuration) exhibit large deviations from experiment and from reliable theoretical results. The spinor averaging (DCHF (av.)) rectifies this problem to a large degree. Including electron correlation effects at up to the level of Double excitations (model SD9_10au) based on the state-averaged spinors diminishes $Q_{zz}(^2D_{3/2})$ by roughly 10% and $Q_{zz}(^2D_{5/2})$ by 8%, respectively. Triple excitations are also not unimportant, further quenching $Q_{zz}(^2D_{3/2})$ and $Q_{zz}(^2D_{5/2})$ by 3 – 4%. The term energies for both excited states are in excellent agreement with experiment in the most accurate model, SDT9_10au, where deviations are less than 1%. Present uncertainties are estimated conservatively to be at most as large as the effect of Triple excitations, accounting for excitation ranks higher than Triples and basis-set truncations.

The present final results fall in between those from Refs. [23] and [24] and are, considering uncertainties, compatible with both. However, from the present series of calculations, it can be concluded that Quadruple excitations and beyond will lead to a further – albeit small – downward correction to Q_{zz} , likely on the order of 1 – 2%.

TABLE I. Atomic electric quadrupole moments and level energies for state k , defined as $\Delta\varepsilon(k) = \varepsilon(k) - \varepsilon(^2S_{1/2})$ with ε the total electronic energy, for Ra^+

Excited state	CI model	$\Delta\varepsilon$ [cm^{-1}]	Q_{zz} [$a.u.$]
$^2D_{3/2}(3d^1)$	DCHF ($7s^1$)	15295	4.944
	DCHF (av.)	13053	3.312
	SD9_10au	12171	2.998
	SDT9_10au	12083	2.879
	Final	12083	2.88(12)
	Other theory		2.84(3)[23]
			2.90(2)[24]
	Exp. [25]	12084.3	
$^2D_{5/2}(3d^1)$	DCHF ($7s^1$)	16021	7.309
	DCHF (av.)	13853	4.964
	SD9_10au	13639	4.559
	SDT9_10au	13654	4.402
	Final	13654	4.40(16)
	Other Theory		4.34(4)[23]
			4.45(9)[24]
	Exp. [25]	13743.0	

A further downward correction of a few percent is to be expected from the inclusion of basis functions with high angular momentum ($\ell > 4$), as has been pointed out in Refs. [23, 26]. The present basis set terminates at $\ell = 4$ for the large-component of the Dirac wavefunctions. Thus, the present EQM results for Ra^+ are in very good agreement with those from Ref. [23] which remain the most accurate to date. This is a further confirmation of the reliability of the present approach to calculating atomic EQMs, which was the goal for this study on Ra^+ .

C. Tm

The afore-going sections have set the stage for making reliable predictions for EQMs in systems where they are so far unknown.

1. Technical details

Two Gaussian basis sets are employed for Tm, Dyall's ccpVTZ set with all $4f$, $6s$, $5s$, $5p$, $5d$ -correlating and $4f$ dipole-polarizing functions added amounting to $\{30s, 24p, 18d, 13f, 4g, 2h\}$

functions and Dyal’s ccpVQZ set including all valence-correlating and the $4f$ dipole-polarizing functions [27], amounting to $\{35s, 30p, 19d, 16f, 6g, 4h, 2i\}$ functions. The Dirac spinors are optimized by diagonalizing a Fock operator where a fractional occupation of $f = \frac{13}{14}$ per spinor with $\ell = 3$ is used ($4f^{13} 6s^2$ ground configuration). Effectively, this yields a Dirac-Hartree-Fock state that is averaged over the ${}^2F_{7/2}$ ground term and the ${}^2F_{5/2}$ excited term and spinors that are not biased towards any of the corresponding states.

TABLE II. Atomic electric quadrupole moments for Tm ${}^2F_{7/2}(4f^{13} 6s^2)$ using various CI models, TZ basis

CI model (number of virtual functions) Q_{zz} [<i>a.u.</i>]	
DCHF	−0.2711
SD15_0.2au (1s, 1d; 2p)	0.1128
SD15_1au (2s, 3d, 1g; 3p, 2f)	−0.0101
SD15_2au (3s, 4d, 2g; 4p, 3f)	−0.1170
SD15_4au (3s, 4d, 2g; 4p, 4f, 1h)	−0.1920
SD15_6au (4s, 5d, 2g; 5p, 5f, 1h)	−0.2319
SD15_10au (4s, 6d, 3g; 5p, 6f, 1h)	−0.2519
SD15_20au (5s, 7d, 3g; 6p, 7f, 1h)	−0.2543
SD15_50au (6s, 8d, 4g; 7p, 8f, 2h)	−0.2530
SD15_130au (7s, 9d, 4g; 8p, 9f, 2h)	−0.2531
SD23_10au	−0.2470
SD33_10au	−0.2473
SDT15_0.2au	0.1181
SDT15_1au	0.0509
SDT15_2au	−0.0139
SDT15_4au	−0.0498
SDT15_6au	−0.0472
SDT15_10au	−0.0299
SDT15_20au	−0.0311
SDT15_50au	−0.0304
SDTQ15_2au	0.021
SDTQ15_4au	0.013
SDTQ15_10au (est.)	0.067

2. Results and discussion

Tables II and III show results for the EQM of the electronic ground term 2F_J . Valence correlation effects from up to Double excitations are converged at the percent level when the virtual spinor space is truncated at 20 *a.u.* These effects decrease Q_{zz} – on the absolute – by about 6%. However, when full Triple excitations are introduced in addition, the EQM is quenched by an astonishing order of magnitude. This strong quenching is basis-set dependent to only about 6% which justifies a deeper investigation using the smaller TZ basis set only.

The strongest positive contribution to Q_{zz} from excitations into the virtual spinor space is observed at the very low cutoff of 0.2 *a.u.* Further cutting down on this virtual set reveals that the positive contribution is mainly due to Double excitations of the type $6s^2 \rightarrow 5d_{5/2,5/2}^2$, the amplitude (CI coefficient) of which diminishes strongly as the dimension of the virtual space is increased. It is remarkable that the residual quenching of Q_{zz} is about +0.24 *a.u.* for the model SDT15_20au which leads to a value for Q_{zz} that is roughly one order of magnitude smaller on the absolute than the DCHF value. Expressed in different terms, we here observe an electron correlation effect (difference between a given CI model and Hartree-Fock theory) of nearly 90% ! This extraordinary situation can be attributed to the fact that the open-*f*-shell contribution to Q_{zz} of the thulium atom is rather small and that even a small amplitude on the contributions that arise from *d*-shell occupations which, furthermore, have opposite sign, can nearly cancel the latter.

The discussed cancellation leads to values for Q_{zz} that are close to zero and thus manifestly very difficult to describe accurately, i.e., with small relative errors. The inclusion of excitation ranks higher than full Triples is explored using the smaller (TZ) basis set, see Table II. Due to the extreme computational demand a truncation of the virtual space has to serve as a further approximation. When this truncation is set to 2 *a.u.* the difference between the models SDT15 and SDTQ15 is +0.034 *a.u.* However, with this spinor space the model SDT15 is qualitatively incorrect. A truncation at 4 *a.u.* yields an SDT15 result that agrees qualitatively with the converged result from SDT15_50au. The corresponding expansion for SDTQ15_4au comprises roughly 6 billion expansion terms, close to the limits of computational feasibility with the current code.

A correction due to full Quadruple excitations – which is not negligible in the present case – is thus obtained as follows. The base value is provided by the model SDT15_10au. Since correlation contributions at any excitation rank are nearly converged at a virtual cutoff of 10 *a.u.* but this spinor space creates a configuration space too large to be treated explicitly when Q excitations are taken into account, the result for the model SDTQ15_10au is estimated by the following formula:

$$Q_{zz}(\text{SDTQ15}_{10\text{au}}) := Q_{zz}(\text{SDT15}_{10\text{au}}) + \Delta Q[Q_{zz}(10\text{au})]$$

where

$$\Delta Q[Q_{zz}(10\text{au})] := (Q_{zz}(\text{SDTQ15_4au}) - Q_{zz}(\text{SDT15_4au})) \times \frac{(Q_{zz}(\text{SDT15_10au}) - Q_{zz}(\text{SD15_10au}))}{(Q_{zz}(\text{SDT15_4au}) - Q_{zz}(\text{SD15_4au}))}$$

This scales the correction due to Quadruple excitations by the ratio of the Triples correction for different virtual cutoff values. In this estimation the assumption is made that the augmentation of the virtual spinor space affects the Triples correction ΔT and the Quadruples correction ΔQ in an equivalent manner. This way of obtaining the correction is also supported by the graphical representation in Fig. (1). ΔT is always positive (as is ΔQ) and increases monotonously as a function of virtual cutoff (assumed for ΔQ). Since the correction due to higher excitation ranks is more than halved when going from ΔT to ΔQ a correction $\Delta 5$ due to full quintuples (or to even higher excitation ranks) is not expected to surpass $+0.05 \text{ a.u.}$ for $Q_{zz}(^2F_{7/2})$.

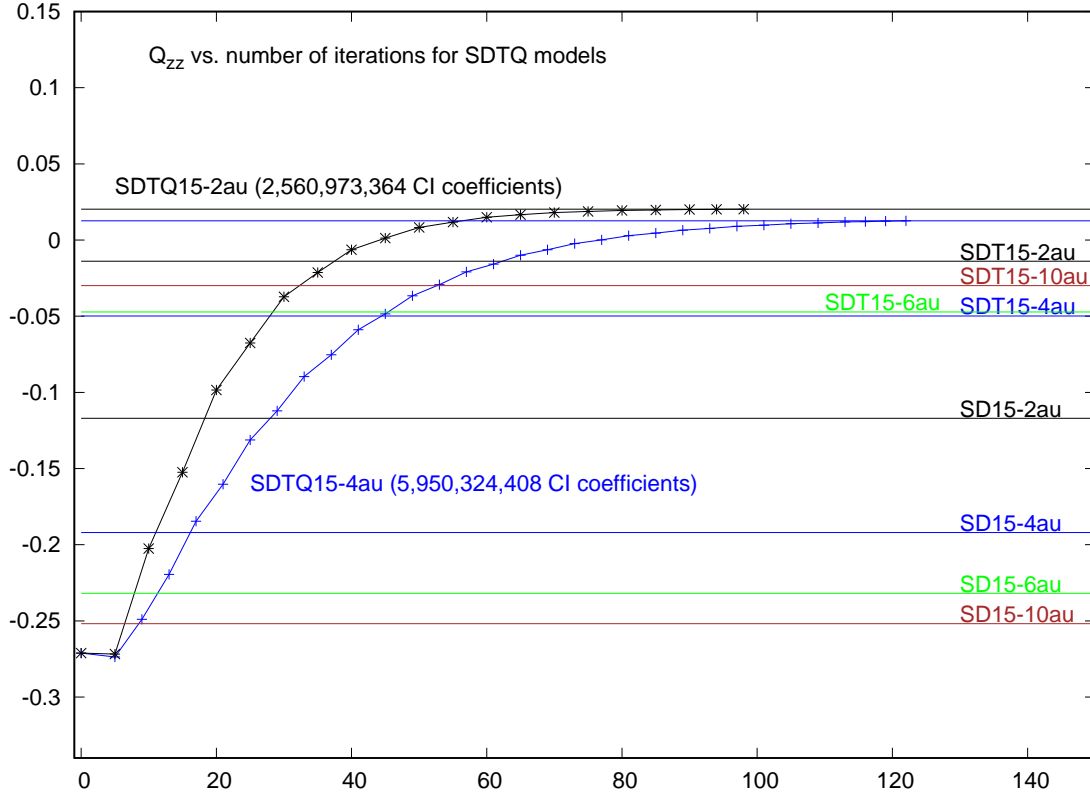
Possible corrections due to the use of the larger QZ basis set are investigated through the calculations presented in Table III. Interestingly, the most elaborate comparable model SDT15_50au does not yield a significant basis-set correction ($\Delta \text{QZ} \approx -0.0001 \text{ a.u.}$). Furthermore, a correction due to core-valence correlation by including single-hole configurations (model S8_SD23_10au) and in addition double-hole configurations (model SD23_10au) in the Tm $5s, 5p$ shells also result in negligibly small corrections. The same is true for correlations due to single- and double-hole configurations in the Tm $4d$ shell (see Table II). The inclusion of additional functions of very high angular momentum (h ($\ell = 5$) and i ($\ell = 6$)) in the basis set does not affect the EQM of the Tm atom appreciably, as can be seen by comparing the models SDT15_50au in Tables II and III. Also, the Triples correction ΔT increases by only about 2.5% when going from the TZ to the QZ basis, a further indication that many-body effects are well described using the TZ basis set.

The present final best result is, therefore, $Q_{zz}(^2F_{7/2}) \approx 0.07 \text{ a.u.}$ I assign to this a rather conservative uncertainty of 100%, almost entirely due to the neglect of higher CI excitation ranks in even the most highly correlated atomic wavefunction (SDTQ). Given the small value of the EQM this uncertainty translates into only 0.07 a.u.

As can be inferred from the above detailed discussion and the results in Table III it can be said with certainty that $0 < Q_{zz}(^2F_{5/2}) < Q_{zz}(^2F_{7/2})$. Thus, the EQM of the electronically excited clock state also has near-zero EQM.

The result by Sukachev et al. [28] obtained with the COWAN code of $Q_{zz}(^2F_{7/2}) \approx 0.5 \text{ a.u.}$ differs from the present final result by roughly 0.4 a.u. This is a large relative and also a significant absolute difference, given the observed discrepancies from different electronic-structure models as compared for the Ra^+ ion in section III B 2 at the highest level of accuracy. The spread of final values for Ra^+ is about an order of magnitude smaller than 0.4 a.u. Since Sukachev et al. do not give any details of their calculation

FIG. 1. EQM (*a.u.*) of $^2F_{7/2}$ Tm ground state using various CI models and virtual cutoffs, TZ basis; horizontal lines display converged values for the respective model. The convergence patterns for the two largest calculations are shown explicitly.



it is not possible to analyze the discrepancy for Tm.

3. Hyperfine interaction

However, a qualitative judgement on the present EQM results is possible in an indirect manner. Since closed-shell contributions to the EQM are zero the spin density in the atomic state is linked to the EQM. The same is true for the magnetic hyperfine interaction constant. Thus, the correlated wavefunctions presently optimized for the description of the Tm EQM are expected to also describe the corresponding hyperfine interaction constant correctly.

Table IV lists the results for A using wavefunctions from the most accurate models for calculating the EQM. The spin density in the correlated wavefunction of the Tm

TABLE III. Atomic electric quadrupole moments and level energies for state k , defined as $\Delta\varepsilon(k) = \varepsilon(k) - \varepsilon(^2F_{7/2})$ with ε the total electronic energy, for Tm using various CI models, QZ basis

State	CI model (virtual functions)	$\Delta\varepsilon$ [cm ⁻¹]	Q_{zz} [<i>a.u.</i>]
$^2F_{7/2}(4f^{13} 6s^2)$	DCHF	0	-0.2711
	SD15_10au (6 <i>s</i> , 5 <i>d</i> , 4 <i>g</i> , 1 <i>i</i> ; 7 <i>p</i> , 7 <i>f</i> , 2 <i>h</i>)	0	-0.2531
	SD15_20au (7 <i>s</i> , 6 <i>d</i> , 5 <i>g</i> , 1 <i>i</i> ; 8 <i>p</i> , 8 <i>f</i> , 3 <i>h</i>)	0	-0.2546
	SD15_50au (8 <i>s</i> , 7 <i>d</i> , 5 <i>g</i> , 2 <i>i</i> ; 9 <i>p</i> , 10 <i>f</i> , 3 <i>h</i>)	0	-0.2556
	SDT15_10au	0	-0.0349
	SDT15_20au	0	-0.0292
	SDT15_50au	0	-0.0305
	S8_SD23_10au	0	-0.2511
	SD23_10au	0	-0.2534
	Exp. [25]	0	
$^2F_{5/2}(4f^{13} 6s^2)$	DCHF	9016	-0.2203
	SD15_5au	9277	-0.1863
	SD15_10au	9215	-0.2059
	SD15_20au	9143	-0.2074
	SDT15_20au	9028	-0.0257
	SD15_50au	9128	-0.2083
	S8_SD23_10au	9199	-0.2043
	SD23_10au	9158	-0.2061
	Exp. [25]	8771.243	

$^2F_{7/2}$ ground state largely resides in f (and d) states which explains why A is comparatively small. Also here the basis set effect is negligibly small. Higher excitations than Triples do not affect A substantially. The result with the largest deviation from the experimental value for A is obtained with the model SDT15_50au/QZ which differs from the experimental value by only about 6.8%. This finding confirms the quality of the wavefunctions used for calculating the EQM in the present work.

IV. CONCLUSIONS AND OUTLOOK

In the present paper an accurate method for the calculation of atomic electronic electric quadrupole moments is presented. The applications to the Be atom and to the Ra⁺ ion demonstrate the reliability of the method.

The quadrupole shift has been identified as one of the contributors to the uncertainty

TABLE IV. Magnetic hyperfine interaction constant A for $^{169}\text{Tm } ^2F_{7/2}(4f^{13}6s^2)$ calculated with Eq. (12) using various CI models and basis sets

CI model/basis set	A [MHz]
SDT15_2au/TZ	-388.5
SDT15_4au/TZ	-391.0
SDT15_6au/TZ	-396.8
SDT15_10au/TZ	-397.5
SDT15_20au/TZ	-399.9
SDT15_50au/TZ	-399.6
SDTQ15_2au/TZ	-388.4
SDTQ15_4au/TZ	-390.8
SDT15_10au/QZ	-397.2
SDT15_20au/QZ	-398.2
SDT15_50au/QZ	-399.5
Exp.[29]	-374.137661(3)

budget for a Tm optical clock using its ground-state fine-structure components [28], albeit not the leading one at the moment. An elaborate, detailed, and high-level study on the Tm atom in the present work shows that the EQM in its $^2F_{7/2}(4f^{13}6s^2)$ ground state is exceptionally small. Thus, the application of methods for systematic cancellation or suppression of the quadrupole shift [30, 31] may not be necessary in a thulium optical clock.

On the methodological side the present work is motivated by the general importance of electric multipole moments and electric transition multipole moments in many areas of atomic and molecular physics. The author has also implemented E1 and E2 transition moments into the present relativistic correlated many-body methods, applications of which will be the subject of publications in the very near future. E1 transition moments allow for the calculation of atomic dispersion coefficients which contribute to a clock's uncertainty through the van der Waals interaction. E2 transition moments are of importance for instance in the field of parity nonconservation [32].

-
- [1] M. S. Safronova, D. Budker, D. DeMille, D. F. Jackson Kimball, A. Derevianko, and C. W. Clark. Search for new physics with atoms and molecules. *Rev. Mod. Phys.*, 90:025008, 2018.
 - [2] A. D. Ludlow, M. M. Boyd, J. Ye, E. Peik, and P. O. Schmidt. Optical atomic clocks. *Rev. Mod. Phys.*, 87:637, 2015.
 - [3] A. Kozlov, V. A. Dzuba, and V. V. Flambaum. Prospects of building optical atomic clocks using Er I or Er III. *Phys. Rev. A*, 88:032509, 2013.
 - [4] A. A. Golovizin, D. O. Tregubov, E. S. Fedorova, D. A. Mishin, D. I. Provorchenko, K. Yu. Khabarova, V. N. Sorokin, and N. N. Kolachevsky. Simultaneous bicolor interrogation in thulium optical clock providing very low systematic frequency shifts. *Nature Communications*, 11:5171, 2021.
 - [5] A. Golovizin, D. Tregubov, D. Mishin, D. Provorchenko, and N. Kolachevsky. Compact magneto-optical trap of thulium atoms for a transportable optical clock. *Opt. Express*, 29:36734, 2021.
 - [6] E. Fedorova, A. Golovizin, D. Tregubov, D. Mishin, D. Provorchenko, V. Sorokin, K. Khabarova, and N. Kolachevsky. Simultaneous preparation of two initial clock states in a thulium optical clock. *Phys. Rev. A*, 102:063114, 2020.
 - [7] A. Golovizin, E. Fedorova, D. Tregubov, D. Sukachev, K. Khabarova, V. Sorokin, and N. Kolachevsky. Inner-shell clock transition in atomic thulium with a small blackbody radiation shift. *Nature Communications*, 10:1724, 2019.
 - [8] S. Knecht, H. J. Aa. Jensen, and T. Fleig. Large-Scale Parallel Configuration Interaction. II. Two- and four-component double-group general active space implementation with application to BiH. *J. Chem. Phys.*, 132:014108, 2010.
 - [9] T. Fleig, H. J. Aa. Jensen, J. Olsen, and L. Visscher. The generalized active space concept for the relativistic treatment of electron correlation. III: Large-scale configuration interaction and multi-configuration self-consistent-field four-component methods with application to UO₂. *J. Chem. Phys.*, 124:104106, 2006.
 - [10] J. D. Jackson. *Klassische Elektrodynamik*. Walter de Gruyter, Berlin, New York, 1983.
 - [11] D. Sundholm and J. Olsen. Finite-element multiconfiguration Hartree-Fock calculations of the atomic quadrupole moments of excited states of Be, Al, In, Ne, Ar, Kr, and Xe. *Phys. Rev. A*, 47:2672, 1993.
 - [12] W. Itano. Quadrupole moments and hyperfine constants of metastable states of Ca⁺, Sr⁺, Ba⁺, Yb⁺, Hg⁺, and Au. *Phys. Rev. A*, 73:022510, 2006.
 - [13] T. Fleig, J. Olsen, and C. M. Marian. The generalized active space concept for the relativistic treatment of electron correlation. I. Kramers-restricted two-component configuration interaction. *J. Chem. Phys.*, 114:4775, 2001.

- [14] T. Fleig, J. Olsen, and L. Visscher. The generalized active space concept for the relativistic treatment of electron correlation. II: Large-scale configuration interaction implementation based on relativistic 2- and 4-spinors and its application. *J. Chem. Phys.*, 119:2963, 2003.
- [15] T. Saue, R. Bast, A. S. P. Gomes, H. J. Aa. Jensen, L. Visscher, I. A. Aucar, R. Di Remigio, K. G. Dyall, E. Eliav, E. Fasshauer, T. Fleig, L. Halbert, E. Donovan Hedegård, B. Helmich-Paris, M. Iliaš, C. R. Jacob, S. Knecht, J. K. Laerdahl, M. L. Vidal, M. K. Nayak, M. Olejniczak, J. M. Haugaard Olsen, M. Pernpointner, B. Senjean, A. Shee, A. Sunaga, and J. N. P. van Stralen. The DIRAC code for relativistic molecular calculations. *J. Phys. Chem.*, 152:204104, 2020.
- [16] Stefan Knecht. *Parallel Relativistic Multiconfiguration Methods: New Powerful Tools for Heavy-Element Electronic-Structure Studies*. Dissertation, Heinrich-Heine-Universität Düsseldorf, Düsseldorf, Germany, 2009.
- [17] E. Wigner. *Group theory and its applications to the quantum mechanics of atomic spectra (English version)*. Academic Press Inc., New York, 1959.
- [18] M. Weissbluth. *Atoms and Molecules*. Academic Press, New York, San Francisco, London, 1978.
- [19] T. Fleig and M. K. Nayak. Electron electric dipole moment and hyperfine interaction constants for ThO. *J. Mol. Spectrosc.*, 300:16, 2014.
- [20] T. Fleig and L. V. Skripnikov. P,T-Violating and Magnetic Hyperfine Interactions in Atomic Thallium. *Symmetry*, 12:498, 2020.
- [21] B. P. Pritchard, D. Altarawy, B. Didier, T. D. Gibson, and T. L. Windus. A New Basis Set Exchange: An Open, Up-to-date Resource for the Molecular Sciences Community. *J. Chem. Inf. Model.*, 59:4814, 2019.
- [22] K. G. Dyall. Relativistic double-zeta, triple-zeta, and quadruple-zeta basis sets for the 4s, 5s, 6s, and 7s elements. *J. Phys. Chem. A*, 113:12638, 2009. (8 pages) *Available online*, DOI: 10.1021/jp905057q. Basis sets available from the Dirac web site, <http://dirac.chem.sdu.dk>.
- [23] R. Pal, D. Jiang, M. S. Safronova, and U. I. Safronova. Calculation of parity-nonconserving amplitude and other properties of Ra^+ . *Phys. Rev. A*, 79:062505, 2009.
- [24] B. K. Sahoo, B. P. Das, R. K. Chaudhuri, D. Mukherjee, R. G. E. Timmermanns, and K. Jungmann. Investigations of Ra^+ properties to test possibilities of new optical frequency standards. *Phys. Rev. A*, 76:040504, 2007.
- [25] A. Kramida, Yu. Ralchenko, J. Reader, and NIST ASD Team. NIST Atomic Spectra Database (ver. 5.9), [Online]. Available: <https://physics.nist.gov/asd> [2022, May 21]. National Institute of Standards and Technology, Gaithersburg, MD., 2021.
- [26] D. Jiang, B. Arora, and M. S. Safronova. Electric quadrupole moments of metastable states of Ca^+ , Sr^+ , and Ba^+ . *Phys. Rev. A*, 78:022514, 2008.

- [27] A. S. P. Gomes, L. Visscher, and K. G. Dyall. Relativistic double-zeta, triple-zeta, and quadruple-zeta basis sets for the lanthanides La–Lu. *Theoret. Chem. Acc.*, 127:369, 2010.
- [28] D. Sukachev, S. Fedorov, I. Tolstikhina, D. Tregubov, E. Kalganova, G. Vishnyakova, A. Golovizin, N. Kolachevsky, E. Kharabova, and V. Sorokin. Inner-shell magnetic-dipole transition in Tm atoms: A candidate for optical lattice clocks. *Phys. Rev. A*, 94:022512, 2016.
- [29] D. Giglberger and S. Penselin. Ground-State Hyperfine Structure and Nuclear Magnetic Moment of Thulium-169. *Z. Phys.*, 199:244, 1967.
- [30] W. Oskay, W. M. Itano, and J. Bergquist. Measurement of the $^{199}\text{Hg}^+ 5d^9 6s^2 \ ^2D_{5/2}$ Electric Quadrupole moment and a Constraint on the Quadrupole Shift. *Phys. Rev. Lett.*, 94:163001, 2005.
- [31] P. Dubé, A. A. Madej, J. E. Bernard, L. Marmet, J.-S. Boulanger, and S. Cundy. Electric quadrupole shift cancellation in single-ion optical frequency standards. *Phys. Rev. Lett.*, 95:033001, Jul 2005.
- [32] Norval Fortson. Possibility of Measuring Parity Nonconservation with a Single Trapped Atomic Ion. *Phys. Rev. Lett.*, 70:2383, 1993.